Original Article

Optimization and comparison of two practical dual-tuned birdcage configurations for quantitative assessment of articular cartilage with sodium magnetic resonance imaging

Gunthard Lykowsky[1,2], Flavio Carinci[1,2], Markus Düring[1,2], Daniel Weber[1], Peter M. Jakob[1,2], Daniel Haddad[1]

[1]MRB Research Center for Magnetic Resonance Bavaria, Wuerzburg, Germany; [2]Department of Experimental Physics 5 (Biophysics), University of Wuerzburg, Wuerzburg, Germany

Correspondence to: Gunthard Lykowsky. MRB Research Center for Magnetic Resonance Bavaria, Am Hubland, Würzburg 97074, Germany. Email: lykowsky@mr-bavaria.de.

Background: In this study, two practical dual-tuned birdcage configurations for quantitative assessment of articular cartilage with sodium magnetic resonance imaging (MRI) were designed and compared.

Methods: Two 1.5 T dual-tuned birdcages, a four-ring birdcage (FRB) and an alternating rungs birdcage (ARB), were built and then characterized by bench and MRI measurements. The relative uniformity (RU) and the efficiency of the coils were compared using ^{23}Na and ^{1}H B_1 maps. *In vivo* images of a volunteer were acquired.

Results: Bench measurements showed matching and decoupling coefficients of the quadrature channels lower than −20 dB. The RUs and 180° pulse amplitudes of the FRB/ARB were determined as: ^{1}H RU =94.4/74.4%, ^{23}Na RU =95.2/93.6%, ^{1}H 180° pulse amplitude =69.2/75.4 V and ^{23}Na 180° pulse amplitude =45.1/45.9 V. The *in vivo* ^{23}Na images acquired with the FRB show a signal-to-noise ratio (SNR) of 6 to 14 in the cartilage.

Conclusions: Due to its superior ^{1}H homogeneity and efficiency and its slightly better ^{23}Na homogeneity, the FRB is the overall preferred coil for the given requirements of this study. The achieved *in vivo* SNR is adequate for quantitative ^{23}Na and high resolution ^{1}H imaging.

Keywords: Sodium magnetic resonance imaging; dual tuned; birdcage

Submitted Oct 01, 2015. Accepted for publication Oct 30, 2015.
doi: 10.3978/j.issn.2223-4292.2015.11.06
View this article at: http://dx.doi.org/10.3978/j.issn.2223-4292.2015.11.06

Introduction

Osteoarthritis (OA) is a degenerative joint disease with a high prevalence in the aging population. The early stages of OA can be associated with a reduction in glycosaminoglycan (GAG) concentration, changes in the size and organization of collagen fibers, and increased water content (1-3). When the disease progresses, morphologic changes like thinning and lesions of the cartilage occur that can be captured by radiography and conventional magnetic resonance imaging (MRI). To maximize the effectiveness of therapeutic approaches to OA, there is high demand for imaging techniques that are sensitive to the early stages of OA. Recently, more advanced MRI techniques have been developed to detect and quantify the early molecular changes that precede the morphological changes of the cartilage. The most popular quantitative MRI techniques of this kind are delayed gadolinium-enhanced magnetic resonance imaging contrast (dGEMRIC) (4,5), $T_{1\rho}$ relaxation mapping (6) and sodium MRI (7-9). Although sodium MR imaging has been shown to strongly correlate with the GAG concentration in the cartilage, its implementation is still challenging because of the low sensitivity of the ^{23}Na nucleus, low *in vivo* concentrations, fast transverse relaxation times and the requirement for x-nuclei compatible scanner hardware and RF coils. Dual-tuned coils provide heteronuclear images and anatomical hydrogen background images without repositioning the

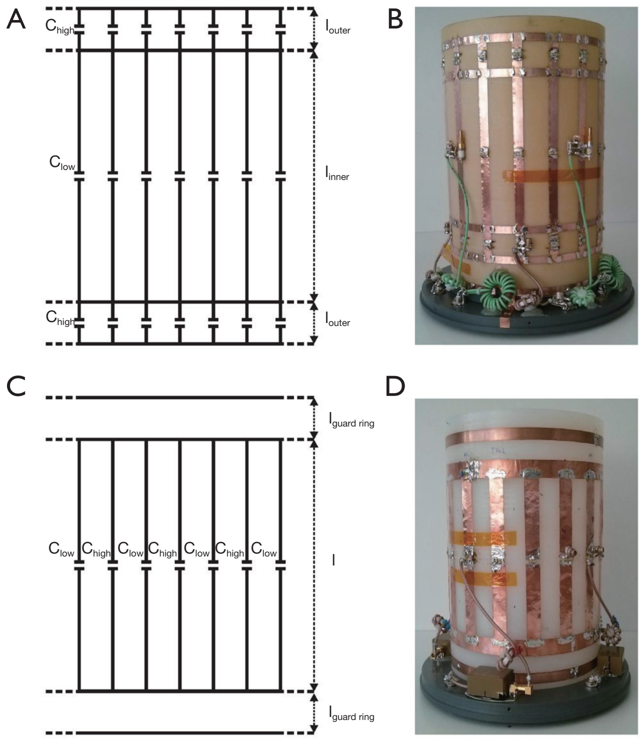

Figure 1 Schematic structures and photographs of the four-ring birdcage (FRB) and the alternating rungs birdcage (ARB). l_{inner} and l_{outer} indicate the length of the inner (sodium) and outer (hydrogen) sections of the FRB (A). l indicates the length of the ARB structure and lguard ring the distance of the guard rings (C). Clow and Chigh indicate the capacitors of the low (sodium) and high (hydrogen) resonance for both, FRB (A) and ARB (C). Photographs of the assembled coils are shown in (B) (FRB) and (D) (ARB).

subject thus avoiding co-registration errors. Furthermore the hydrogen channel can be used for efficient B_0 shimming, which is often required in heteronuclear imaging applications.

Due to the anatomy of the human leg, the birdcage with its cylindrical structure is well suited to perform imaging of the knee joint. Several approaches to achieve dual tuning of a birdcage structure have been proposed over the years: double tuning LC circuits on rungs (10), filters on rungs (11,12), concentric birdcages (13), four-ring birdcages (14) and birdcages with alternating low and high frequency tuned rungs (15,16). All of these designs have their advantages and weaknesses in regard to B_1 field homogeneity, coil efficiency, complexity and geometric requirements. Generally, inserting tank circuits or filters into the coil structure to facilitate dual tuning is cumbersome and leads to additional losses which might be unacceptable at the low gamma nucleus. In contrast two designs, the four-ring birdcage (FRB) (14) and the alternating rungs birdcage (ARB) (15) are especially attractive under practical considerations since they combine both frequency modes in one easy-to-build structure, but don't require additional lossy dual tuning circuits. Thus the efficiency of the low gamma nucleus is only slightly degraded compared to a single-tuned coil. To find a practical and well performing coil for future sodium and hydrogen MRI studies of the human knee, a FRB and ARB coil were designed and then characterized using workbench and MRI measurements.

Methods

Coil structures

Four-ring birdcage (FRB)

The 1.5 T ^{23}Na/^{1}H dual-tuned FRB coil consists of three connected, low-pass birdcages with 16 legs (*Figure 1A,B*). The inner ^{23}Na birdcage is tuned at 16.8 MHz with the central capacitors C_{low} and acts very similar to a single-tuned low-pass birdcage. The outer birdcages are tuned with capacitors C_{high} and couple through space and through the rungs to provide together a homogenous ^{1}H mode at 63.6 MHz. A drawback often encountered with FRB structures is the increase of the axial coil length due to the outer birdcage structures. The diameter of the human thigh is considerable bigger than the diameter of the knee and the calf, thus a long coil makes it difficult to place the knee in the center of the coil without increasing the diameter of the coil. This would be detrimental to the coil efficiency due to a decreased filling factor. Additionally the increased length might cause patient discomfort. Duan *et al.* (17) computationally optimized the lengths of the FRB structure while taking these geometric considerations, field homogeneity and coil efficiency of both nuclei into account. Considering these simulations, the lengths of the inner and outer birdcage were set to 15 cm (l_{inner}) and 2.5 cm (l_{outer}) for the 18 cm diameter coil built in this study.

Alternating rungs birdcage (ARB)

The 1.5 T ^{23}Na/^{1}H dual-tuned ARB coil consists of a low-pass birdcage with 16 rungs which are alternatingly populated with capacitors C_{low} and C_{high} to resonate the coil at 16.8 MHz and 63.6 MHz (*Figure 1C,D*). The length l of 15 cm and the diameter of 18 cm of the ARB were chosen to provide the same ^{23}Na FOV as the FRB.

Table 1 Capacitor values of the four-ring birdcage (FRB) and the alternating rungs birdcage (ARB)

Capacitor (pF)	FRB	ARB
C_{low}	32.2	68.5
C_{high}	213.0	406.8

Materials

For both birdcage coils formers with 18 cm diameter were chosen to comfortably fit around a human knee. Some commercial knee coils can be split in two halves to allow easier patient access (18). This complicates the coil construction process and introduces additional connector losses and coil asymmetries. Thus it was decided to build the coils on closed cylinders. The diameter of 18 cm of the coils built for this study allows accessing the coils by slightly flexing the ankle which was found unproblematic. The coil structures were constructed with adhesive-back copper strips (3M, St. Paul, MN, USA) with a thickness of 35 µm. Coaxial HF-shields with a diameter of 24 cm were used to minimize the interaction of the coils with the scanner bore and avoid aliasing from the other leg. Non-magnetic capacitors (TEMEX Ceramics, Pessac, France) and variable trimmer capacitor (Voltronics, Denville, NJ, USA) were used to tune the coils.

Bench tests

An Agilent (Santa Clear, CA, USA) E5071B vector network analyzer was used to measure the S-parameters and resonance patterns.

Tuning

The capacitors required to resonate the FRB and ARB at the desired frequencies can be calculated by the equations provided in (14) and (15). In practice it is sufficient to start by calculating the capacitors needed for a single-tuned low pass birdcage at the ^{23}Na frequency. The additional ^{1}H tuning rungs with their low capacitance represent high impedance at the ^{23}Na frequency and therefore have little influence on the tuning of the ^{23}Na mode. In contrast, the capacitors of the ^{23}Na structure represent low impedance, i.e., almost shorts at the ^{1}H frequency. Thus, tuning of the ^{1}H and ^{23}Na modes is a largely independent procedure. The final capacitor values are listed in *Table 1*. To suppress gradient eddy currents, two equally spaced 100 nF bypass capacitors were added per end ring (19).

Matching and interfacing

Both coils were capacitively matched to 50 Ohm with symmetric networks. Both nuclei are driven in quadrature with custom-built quadrature hybrids. Cable traps and low/high-pass filters in the feed lines tuned to the appropriate frequencies were incorporated to ensure coil safety and stability.

MR experiments

All MR experiments were performed on a 1.5 T clinical scanner (Siemens Medical Solutions, Erlangen, Germany) with x-nuclei capability.

Acquisition of B_1 maps

A cylindrical phantom (11 cm diameter) containing a saline water solution (5 g/L NaCl and 1.25 g/L $NiSO_4$) was used to characterize the coils. B_1 mapping was performed on both nuclei to assess the coil homogeneity and efficiency. To obtain high quality sodium B_1 maps a phase-sensitive method (20,21) with a 3D gradient echo (GRE) readout (resolution 5×5×10 mm^3, TE: 7 ms, TR: 100 ms, Bandwidth: 80 Hz/pixel, TA: 35:00 min) was used. The B_1 field of the ^{1}H channel was mapped with a 3D GRE sequence with a Bloch-Siegert shift (22) preparation (resolution 5×5×5 mm^3, TE: 7 ms, TR: 20 ms, Bandwidth: 250 Hz/pixel, TA: 0:45 min).

Evaluation of the B_1 field homogeneity, efficiency and signal-to-noise ratio (SNR)

To quantitatively evaluate the field homogeneity the relative uniformity (RU) within the central FOV (11 cm diameter, 8 cm length) of the B_1 maps was calculated. RU represents the percentage of pixels inside the FOV whose relative deviation is not bigger than 10% of the mean B_1 field $\overline{B_1}$ Eq. [1] (23):

$$\mathrm{RU}=\frac{\text{Number of pixels with } \frac{B_1-\overline{B_1}}{B_1}\times 100>10)\times 100}{\text{Total number of pixels}} \quad [1]$$

The B_1 maps were also used to calculate the required voltage amplitude for a 180° block pulse of 1 ms length at the center of the coil. This voltage serves as a measure of the coil efficiency and SNR since B_1 is direct proportional to the SNR (24).

In vivo imaging

In vivo data of a volunteer was acquired with the FRB to verify that the coil performance is sufficient to perform sodium and hydrogen imaging of the human knee. For ^{1}H imaging a high resolution 3D MEDIC (multi-echo data imaging

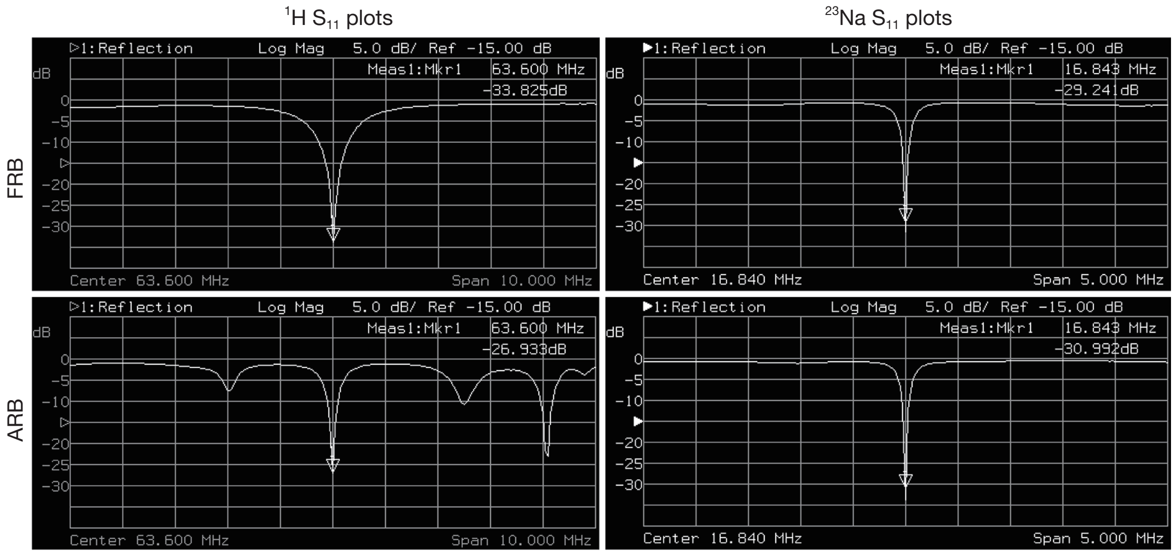

Figure 2 S11 plots of the four-ring birdcage (FRB) and the alternating rungs birdcage (ARB) for ^{1}H (span 10 MHz) and ^{23}Na (span 5 MHz) in dB. All plots show well-defined resonance modes with sufficient mode separation.

Table 2 ^{23}Na and ^{1}H bench measurements of the coupling and matching coefficients of the four-ring birdcage (FRB) and the alternating rungs birdcage (ARB) in dB

Nucleus	Quantity (dB)	FRB	ARB
^{23}Na	Match	–29	–28
	Isolation	–31	–29
	^{1}H coupling	–42	–43
^{1}H	Match	–31	–25
	Isolation	–26	–21
	^{23}Na coupling	–32	–31

combination) sequence (resolution: 0.47×0.51×1.5 mm^3, TR: 37 ms, TE: 20 ms, flip angle: 20°, TA: 8 min) was used. For ^{23}Na imaging a 3D GRE dataset was acquired (resolution: 2.7×2.7×8 mm^3, TR: 11.4 ms, TE: 4 ms, Bandwidth: 85 Hz/pixel, TA: 30 min). The *in vivo* SNR is given as the signal intensity of each pixel divided by the standard deviation of the noise of the background.

Results

After building the structures of the FRB and the ARB the coils were tuned, matched and their coupling coefficients were determined with the cylindrical phantom. *Figure 2* shows the S_{11} plots of the FRB and ARB for ^{1}H (span 10 MHz) and ^{23}Na (span 5 MHz) in dB after tuning and matching the coil. All plots show well-defined resonance modes with sufficient mode separation. The worst case coupling coefficients can be found in *Table 2*. The goal to sufficiently match and isolate the ^{23}Na and ^{1}H channels was achieved without complications. To further increase the isolation between the ^{1}H and ^{23}Na channels to at least 20 dB, filters were added to the ^{23}Na feed lines on both coils and ^{23}Na filters on the ARB. For the FRB the least inter nuclei coupling was observed when the ^{1}H and ^{23}Na channels were 45° apart.

The acquired B_1 maps (*Figure 3*) were used to calculate the RU and the 180° pulse amplitude (*Table 3*). The ^{23}Na efficiencies of the two coils are almost identical (45.1 *vs.* 45.9 V) while the RU of the FRB is slightly higher (95.2% *vs.* 93.6%) than the ARB's. Regarding the ^{1}H performance the FRB outperforms the ARB at both efficiency (69.2 *vs.* 75.4 V) and field homogeneity (94.4% *vs.* 74.4%).

As results of the better performance in the phantom measurements, the FRB was chosen to acquire *in vivo* data of a volunteer. *Figure 4* shows a sagittal slice of the acquired morphological 3D MEDIC data set and the 3D sodium data set. Additionally an overlay image of the segmented ^{23}Na cartilage signal onto the ^{1}H image was created. The ^{23}Na SNR of the cartilage is in the range of 6 to 14.

Discussion

Two practical dual-tuned quadrature birdcages for the

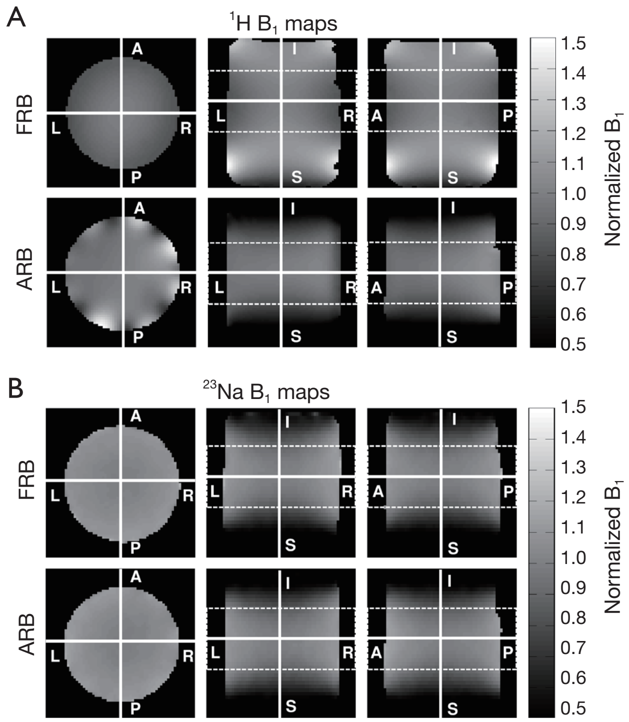

Figure 3 Orthogonal slices of the normalized 3D B_1 maps of the four-ring birdcage (FRB) and the alternating rungs birdcage (ARB). The images correspond to axial, coronal and sagittal slices (from left to right) of the 3D B_1 ^{1}H (A) and ^{23}Na B_1 datasets (B). The labels on the images indicate the physical orientation of the B_1 maps: top-to-bottom (A-P), left-to-right (L-R), and front-to-back (I-S). The dashed lines mark the volume used for the calculation of the relative uniformity (RU).

Table 3 Relative uniformities (RU) of the central FOV in percent and 180° pulse amplitudes in Volt of the four-ring birdcage (FRB) and the alternating rungs birdcage (ARB) for ^{1}H and ^{23}Na

Nucleus	Quantity	FRB	ARB
^{23}Na	RU (%)	95.2	93.6
	180° pulse amplitude (V)	45.1	45.9
^{1}H	RU (%)	94.4	74.4
	180° pulse amplitude (V)	69.2	75.4

human knee were designed and characterized. Both coils show well-defined resonance modes and the bench measurements of the matching and decoupling coefficients were well within the commonly accepted requirements (<–20 dB). Sodium and hydrogen B_1 maps were acquired to investigate the efficiency and RF field homogeneity of the coils. As expected the ^{23}Na efficiency of the FRB and the ARB is almost identical since the additional ^{1}H rungs have little influence on the ^{23}Na currents. The field homogeneity of a birdcage coil increases with its number of rungs. Correspondingly, the FRB with its 16 rungs is superior in field homogeneity to the ARB with its eight rungs contributing to the ^{23}Na field as indicated by the lower RU. The imaging coverage of ^{1}H and ^{23}Na in the axial direction is identical for the ARB (*Figure 3*). Unlike, the FRB's axial imaging coverage for ^{1}H is considerably larger than for ^{23}Na due to the longer length of the ^{1}H structure (19 *vs.* 15 cm). This might be causing aliasing in

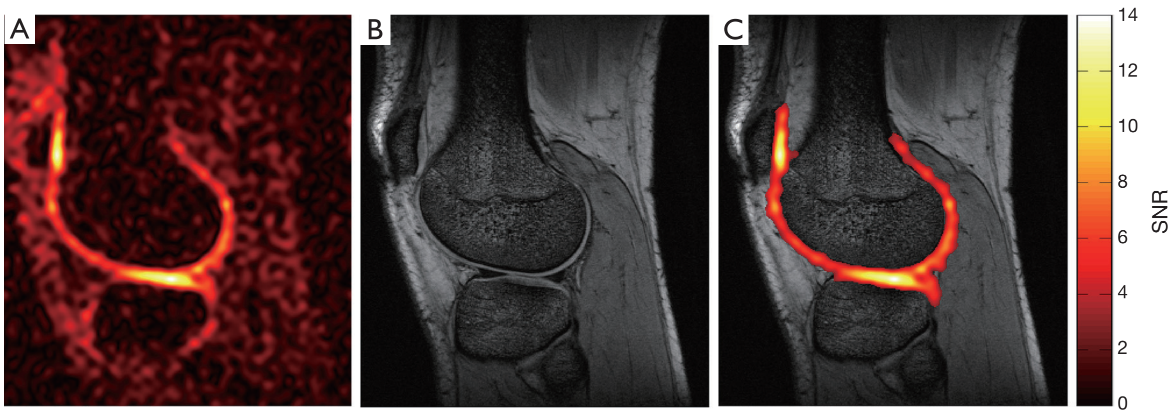

Figure 4 Sagittal images of a ^{23}Na and ^{1}H *in vivo* dataset acquired with the four-ring birdcage (FRB) coil. From left to right: ^{23}Na image (A), ^{1}H image (B) and overlay of the color-mapped ^{23}Na signal-to-noise ratio (SNR) of the cartilage onto the ^{1}H image (C). The colorbar indicates the SNR of the ^{23}Na image.

the axial direction, if not addressed properly during image acquisition. The ^{23}Na rungs of the ARB support counter rotating currents at the ^{1}H frequency that have a negative impact on the ^{1}H field homogeneity. This effect is visible as periodic B_1 field attenuations near the rungs (*Figure 3A*). Accordingly, the FRB is superior to the ARB regarding the ^{1}H field homogeneity and efficiency. The achieved *in vivo* resolution and SNR of the sodium images acquired with the FRB allow quantification of the sodium concentration of the cartilage as shown by others researchers (18). High resolution anatomical ^{1}H images could be obtained without averaging.

Conclusions

Concluding, the ARB and FRB are both practical dual-tuned coils and deliver similar ^{23}Na efficiency. Due to its superior ^{1}H homogeneity and efficiency and its slightly better ^{23}Na homogeneity, the FRB is the overall preferred coil for the given requirements of this study.

Acknowledgements

Funding: This work was funded by the EU as part of the Seventh Framework Program (FP7) in the Health project 241719 "ADIPOA".

Footnote

Conflicts of Interest: The authors have no conflicts of interest to declare.

References

1. Bollet AJ, Nance JL. Biochemical Findings in Normal and Osteoarthritic Articular Cartilage. II. Chondroitin Sulfate Concentration and Chain Length, Water, and Ash Content. J Clin Invest 1966;45:1170-7.
2. Rizkalla G, Reiner A, Bogoch E, Poole AR. Studies of the articular cartilage proteoglycan aggrecan in health and osteoarthritis. Evidence for molecular heterogeneity and extensive molecular changes in disease. J Clin Invest 1992;90:2268-77.
3. Pearle AD, Warren RF, Rodeo SA. Basic science of articular cartilage and osteoarthritis. Clin Sports Med 2005;24:1-12.
4. Bashir A, Gray ML, Burstein D. Gd-DTPA2- as a measure of cartilage degradation. Magn Reson Med 1996;36:665-73.
5. Bashir A, Gray ML, Boutin RD, Burstein D. Glycosaminoglycan in articular cartilage: in vivo assessment with delayed Gd(DTPA)(2-)-enhanced MR imaging. Radiology 1997;205:551-8.
6. Duvvuri U, Reddy R, Patel SD, Kaufman JH, Kneeland JB, Leigh JS. T1rho-relaxation in articular cartilage: effects of enzymatic degradation. Magn Reson Med 1997;38:863-7.
7. Reddy R, Insko EK, Noyszewski EA, Dandora R, Kneeland JB, Leigh JS. Sodium MRI of human articular cartilage in vivo. Magn Reson Med 1998;39:697-701.
8. Shapiro EM, Borthakur A, Gougoutas A, Reddy R. 23Na MRI accurately measures fixed charge density in articular cartilage. Magn Reson Med 2002;47:284-91.
9. Wheaton AJ, Borthakur A, Shapiro EM, Regatte RR, Akella SV, Kneeland JB, Reddy R. Proteoglycan loss in human knee cartilage: quantitation with sodium MR imaging--feasibility study. Radiology 2004;231:900-5.
10. Isaac G, Schnall MD, Lenkinski RE, Vogele K. A design for a double tuned birdcage coil for use in an integrated MRI/MRS examination. J Magn Reson 1990;89:41-50.
11. Rath AR. Design and performance of a double-tuned birdcage coil. J Magn Reson 1990;86:488-95.
12. Matson GB, Vermathen P, Hill TC. A practical double-tuned 1H/31P quadrature birdcage headcoil optimized for 31P operation. Magn Reson Med 1999;42:173-82.
13. Fitzsimmons JR, Beck BL, Brooker HR. Double resonant quadrature birdcage. Magn Reson Med 1993;30:107-14.
14. Murphy-Boesch J, Srinivasan R, Carvajal L, Brown TR. Two configurations of the four-ring birdcage coil for 1H imaging and 1H-decoupled 31P spectroscopy of the human head. J Magn Reson B 1994;103:103-14.
15. Amari S, Uluğ AM, Bornemann J, van Zijl PC, Barker PB. Multiple tuning of birdcage resonators. Magn Reson Med 1997;37:243-51.
16. Wang C, Li Y, Wu B, Xu D, Nelson SJ, Vigneron DB, Zhang X. A practical multinuclear transceiver volume coil for in vivo MRI/MRS at 7 T. Magn Reson Imaging 2012;30:78-84.
17. Duan Y, Peterson BS, Liu F, Brown TR, Ibrahim TS, Kangarlu A. Computational and experimental optimization of a double-tuned (1)H/(31)P four-ring birdcage head coil for MRS at 3T. J Magn Reson Imaging 2009;29:13-22.
18. Hani AF, Kumar D, Malik AS, Razak R. Physiological assessment of in vivo human knee articular cartilage using sodium MR imaging at 1.5 T. Magn Reson Imaging 2013;31:1059-67.
19. Shen GX, Boada FE, Thulborn KR. Dual-frequency, dual-quadrature, birdcage RF coil design with identical B1

pattern for sodium and proton imaging of the human brain at 1.5 T. Magn Reson Med 1997;38:717-25.
20. Morrell GR. A phase-sensitive method of flip angle mapping. Magn Reson Med 2008;60:889-94.
21. Allen SP, Morrell GR, Peterson B, Park D, Gold GE, Kaggie JD, Bangerter NK. Phase-sensitive sodium B1 mapping. Magn Reson Med 2011;65:1125-30.
22. Sacolick LI, Sun L, Vogel MW, Dixon WT, Hancu I. Fast radiofrequency flip angle calibration by Bloch-Siegert shift. Magn Reson Med 2011;66:1333-8.
23. Garrido Salmon CE, Géa Vidoto EL, Martins MJ, et al. Optimization of saddle coils for magnetic resonance imaging. Braz J Phys 2006;36:4-8.
24. Hoult DI, Richards RE. The signal-to-noise ratio of the nuclear magnetic resonance experiment. J Magn Reson (1969) 1976;24:71-85.

Cite this article as: Lykowsky G, Carinci F, Düring M, Weber D, Jakob PM, Haddad D. Optimization and comparison of two practical dual-tuned birdcage configurations for quantitative assessment of articular cartilage with sodium magnetic resonance imaging. Quant Imaging Med Surg 2015;5(6):799-805. doi: 10.3978/j.issn.2223-4292.2015.11.06